ELSEVIER

Desalination 147 (2002) 417–423

DESALINATION

www.elsevier.com/locate/desal

High-flux palladium-silver alloy membranes fabricated by microsystem technology

F.C. Gielens[a]*, H. D. Tong[b], C.J.M. van Rijn[c], M.A.G. Vorstman[a], J.T.F. Keurentjes[a]

[a]*Department of Chemical Engineering and Chemistry, Process Development Group, Eindhoven University of Technology, P.O. Box 513, 5600 MB Eindhoven, The Netherlands*
Tel. +31 (40) 2474956; Fax +31 (40) 2446104; email: f.c.gielens@tue.nl
[b]*MESA+ Research Institute, University of Twente, P.O. Box 217, 7500 AE, Enschede, The Netherlands*
[c]*Aquamarijn Micro Filtration B.V., Beatrixln. 2, 7255 DB, Hengelo, The Netherlands*

Received 7 February 2002; accepted 4 April 2002

Abstract

In this study, hydrogen selective membranes have been fabricated using microsystem technology. A 750 nm dense layer of Pd (77 wt%) and Ag (23 wt%) is deposited on a non-porous 1 mm thick silicon nitride layer by co-sputtering of a Pd and a Ag target. After sputtering, openings of 5 μm are made in the silicon nitride layer to create a clear passage to the Pd/Ag surface. As a result of the production method, these membranes are pinhole free and have a low resistance to mass transfer in the gas phase, as virtually no support layer is present. The membranes have been tested in a gas permeation system to determine the hydrogen permeability as a function of temperature, gas flow rate, and feed composition. In addition, the hydrogen selectivity over helium has been determined, which appears to be above 1500. At 0.2 bar partial hydrogen pressure in the feed, the hydrogen permeability of the membranes has been found to range from 0.02 to 0.95 mol.H_2/m^2×s at 350 and 450°C, respectively. It is expected that by improving the hydrodynamics and increasing the operation temperature, substantially higher fluxes will be attainable.

Keywords: Hydrogen permeation; Palladium alloys; Microsieve; Micro-membrane; Micro-reactor

1. Introduction

The yield of the dehydrogenation of alkanes to alkenes can significantly be increased by using a Pd or Pd/Ag membrane reactor for the selective removal of the hydrogen formed [1–4]. For this purpose, the membrane can either be applied in a direct combination with the reaction in a membrane reactor or as membrane modules placed between a series of reactors. To operate both units economically, it is necessary to have a highly permeable

*Corresponding author.

Presented at the International Congress on Membranes and Membrane Processes (ICOM), Toulouse, France, July 7–12, 2002.

PII: S0011-9164(02)00637-9

hydrogen selective membrane with a high membrane area per volume [5]. In the last decade, a substantial research effort has been focused on achieving higher fluxes by depositing thin Pd or Pd/Ag membranes on porous support materials and to increase the membrane area per volume [6]. However, at these large fluxes the support layer becomes limiting, both in the case a sweep gas is used or when a vacuum is applied at the permeate side [7]. In addition, the permselectivity is often poor, as during the deposition of the Pd(Ag) layer the pores of the support are not well covered by the Pd(Ag) layer [8]. This is probably due to the fact that the Pd(Ag) has a tendency to deposit on top of the support material or on top of the previously deposited layer, and not to enter the pores. As a result, pin-holes are formed.

To overcome these problems (a limiting support layer and the formation of pin-holes), in this study a membrane is made with an ultra-thin support layer using microsystem technology. The advantage of the applied fabrication method is that first the Pd/Ag film is deposited on a silicon wafer which is non-porous, thus resulting in a pin-hole free Pd/Ag film. In addition, the micro-scale of the membrane package insures a low gas phase resistance compared to a porous support.

2. Experimental

2.1. Membrane fabrication with microsieve and packaging

Pd/Ag membranes were prepared as follows. A double-side polished silicon substrate (110), 3 inch in diameter and 350 μm thick, was coated with 0.3 μm of wet-thermally oxidized SiO_2 (Fig. 1). The SiO_2 coating serves as a protective layer during subsequent etching steps. On top of the SiO_2 coating a strong Si_xN_y (low stress silicon-rich silicon nitride) layer was deposited by LPCVD. The Si_xN_y layer is serving as a thin support layer for the Pd/Ag that will be deposited in a later stadium. Parallelogram-shaped structures of 350 by 2100 μm were imprinted on one side of the Si_xN_y layer by standard photo-lithography, followed by etching the Si_xN_y and SiO_2. Then the wafer was immersed in a KOH solution to etch

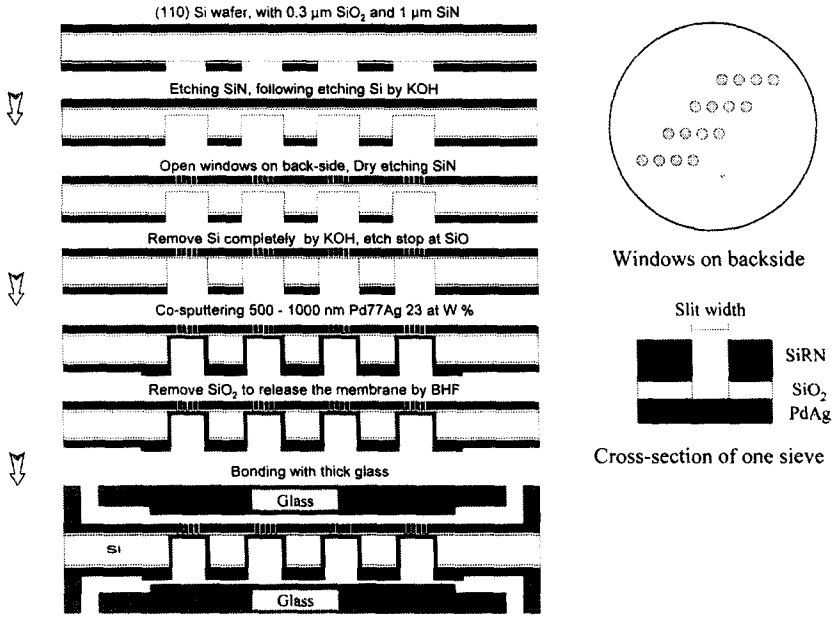

1. Membrane fabrication process.

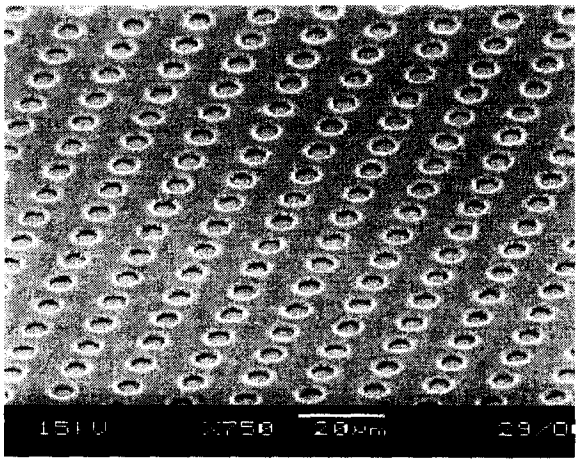

Fig. 2. Microsieve side of the membrane before bonding.

slits in the silicon to a depth of 300 μm (50 μm of silicon is left). At the other side of the wafer circular openings of 5 μm were imprinted on the Si_xN_y layer, followed by dry etching of the Si_xN_y layer, thus creating the microsieve (Fig. 2). Subsequently, the wafer was etched again with a KOH solution to remove the remaining 50 μm Si in the parallelogram-shaped slits. After the SiO_2 layer was reached, an alloy layer of Pd/Ag (77/23 wt.%) with a thickness ranging from 0.5 to 1 μm was deposited by co-sputtering [9] through a shadow mask inside the parallelogram-shaped slits, using titanium (Ti) as an adhesion layer. Next, the SiO_2 in the 5 μm openings in the Si_xN_y was removed by etching the microsieve side with BHF to reveal the membrane surface. A more detailed description is given by Tong et al. [10]. The effective membrane area per unit volume is approximately 200 m^2/m^3.

The silicon wafer was bonded between two thick glass wafers by a four-electrode anodic bonding (bottom of Fig. 1). Prior to the bonding procedure, flow channels of 200 μm depth were created by powder blasting in each of the two 5 mm thick glass wafers. The flow channels start and end at previously drilled holes through the glass wafers.

2.2. Membrane characterization

The morphology of the Pd/Ag surface was studied by scanning electron microscope (Jeol JSM-5600) before and after applying hydrogen. It was not possible to use one single membrane for both, as it was necessary to destroy the glass plates to be able to inspect the membrane surface. The thickness of the membranes was determined by using a Dektak surface profiler and SEM.

The permeability of the membrane was determined for H_2 and He with the experimental setup shown in Fig. 3. Nitrogen was used as a sweep gas at the permeate side. All feed flow rates were measured and controlled with mass flow controllers (Bronkhorst High-Tec, EL-FLOW). The permeate pressure was measured and controlled

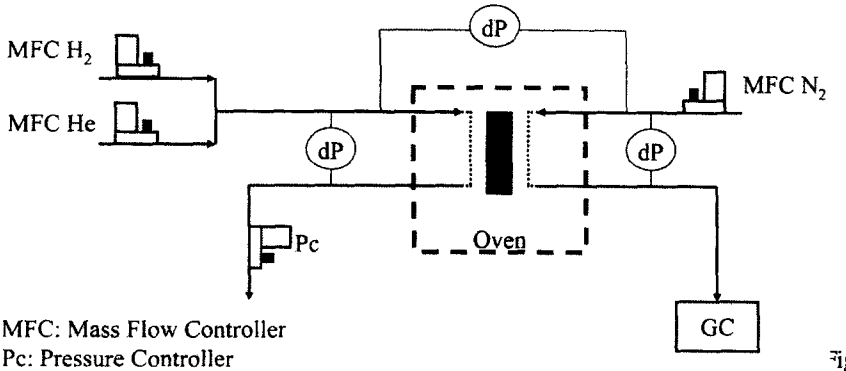

MFC: Mass Flow Controller
Pc: Pressure Controller
GC: Gas Chromatograph

Fig. 3. Schematic view of experimental set-up.

with an absolute pressure controller (Bronkhorst High-Tec, EL-PRESS). The trans-membrane pressure, the pressure drop over the permeate side, and the pressure drop over the retentate side were also measured (Hottinger Baldwin Messtechnik, PD1). A temperature-controlled oven was used to ensure isothermal operation. The H_2 and He concentrations in the permeate were measured by a GC equipped with a TCD detector and a molsieve 5 Å column. Argon was used as the carrier gas, which gives the TCD a high sensitivity to H_2 and He, and a poor sensitivity to N_2. The purity of all gases used was 5.0.

The membrane package was placed in a stainless steel holder, in which graphite rings were used to seal the gas connections between the glass plates and holder. The membrane holder was placed in the oven for isothermal operation and both the H_2/He feed and the sweep gas were preheated in spirals placed in the same oven. The permeation experiments were carried out at 350, 400 and 450°C, respectively. The feed flow was varied between 300 and 1000 ml/min and the H_2 molar fraction was varied from 0.1 to 0.3 mol/mol. The sweep gas flow was kept constant at 300 ml/min.

The experimental set-up was controlled by a PLC. A PC with Labview handled the data-acquisition at 100 Hz. The set-up was running fully automatic 24 h/d, and could handle 100 recipes without user intervention. For each recipe, 4 samples per hour were taken of the permeate that were analyzed by GC.

Before a permeation experiment was started, the membrane was activated for four hours at a temperature of 450°C. During activation a flow of 20 mol% H_2 in He was fed to the retentate and permeate side of the membrane. After activation pure He was fed to the retentate side and pure N_2 to the permeate side. A trans-membrane pressure of 50 mbar was applied and 4 samples were taken to detect any He leak through the membrane. Subsequently, the H_2 permeation experiment could be started.

3. Results and discussion

In Fig. 4, SEM pictures of the Pd/Ag surface in the slit are given. Measurements of the membrane thickness by the surface profiler gave a value of 750 nm, which is confirmed by SEM pictures of a cross section of the membrane.

The picture on the left is a pristine membrane, and on the right a membrane that has been used for permeation experiments is shown. After the permeation experiments, the morphology of the Pd/Ag layer is changed at well-defined circular areas. The position and shape of the areas in which the Pd/Ag is changed to a more coarse grain

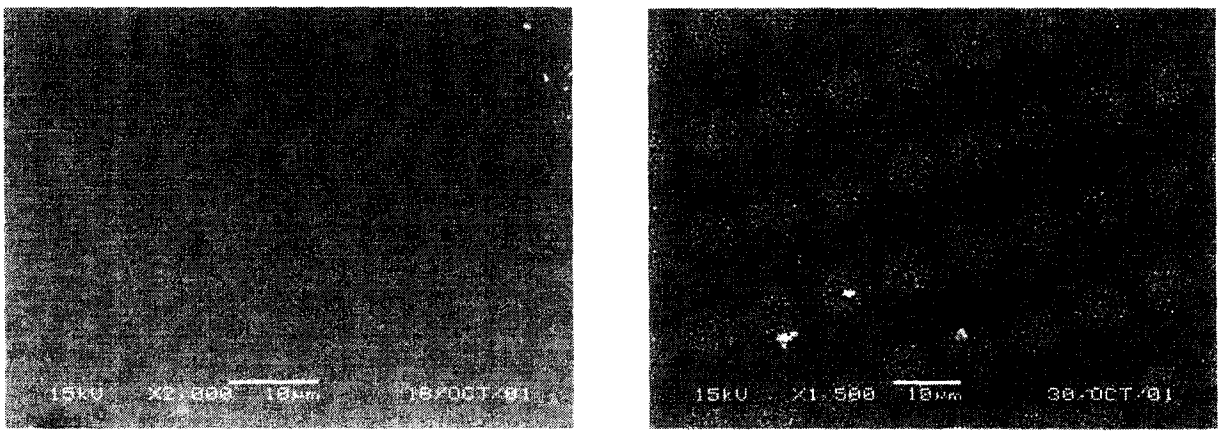

Fig. 4. Pd/Ag surface in the slit: left picture is taken from a pristine membrane, right picture is taken after experiments.

structure reveals that these areas are exactly above the openings in the microsieve. Remarkable is that the diameter of the areas with the structure change is significantly larger than the diameter of the microsieve opening. At the microsieve side, however, there are no visible changes in the Pd/Ag layer after the permeation experiments.

In Fig. 5, the hydrogen permeability is given as a function of temperature and time. The feed and sweep gas flow rates have been kept constant at 300 ml/min. Three series of measurements have been carried out with one single membrane of 750 nm thickness. Within each series the following temperature order was used: 450, 350, 400°C. Series one was measured directly after activation, series two was measured 80 h after the end of series one, and series three 55 h after the end of series 2. At 350°C, the H_2 permeability is one decade higher for the first series compared to the other two, while at 400 and 450°C the H_2 permeabilities are in the same order of magnitude. Initially, it seems that the permeation is limited by atomic diffusion (series 1), whereas the transport is limited by surface processes later (series 2 and 3) [11]. An explanation might be that at the start of the permeation experiment the Ag content in Pd/Ag layer is homogeneous (measured with XPS [10]), but due to the presence of H_2 and elevated temperatures the Ag migrates from the membrane bulk to the membrane surface.For a Pd/Ag sample placed in vacuum and at 400°C Kuijers and Ponec [12] found a Pd surface composition of 8 times lower than the bulk composition. Shu et al. [13] also found surface segregation for a Pd/Ag membrane but not to that degree, we expect that equilibrium between surface and bulk composition was not yet reached in their experiments. The increase of Ag at the surface would cause a decrease in the number of active sites necessary for the H_2 dissociation and association reactions.

At 400°C, an experiment has been performed with a variation in the hydrogen fraction in the feed from 0.1 to 0.3 mol/mol, at a feed flow rate of 1000 ml/min (Fig. 6). The hydrogen flux depends linearly on the driving force ($p_{H2\ retentate} - p_{H2\ permeate}$). Since this is not according to Sieverts law, the flux is not limited by atomic diffusion. The linear dependency on hydrogen concentration is in agreement with the explanation given above for the change in permeation limitation.

To determine the influence of the mass transfer resistance in the gas phase on the overall H_2 permeability, the feed flow rate has been varied between 300 and 1000 ml/min, while the other variables are

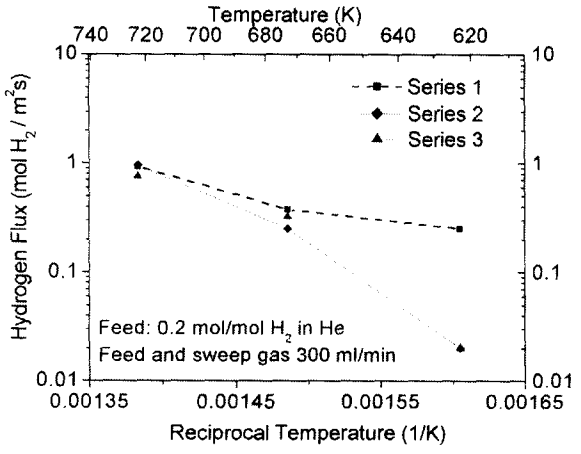

Fig. 5. Hydrogen permeability as function of temperature and time.

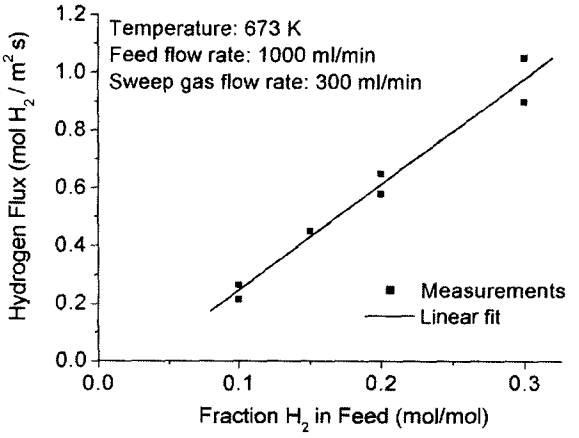

Fig. 6. Hydrogen permeability as function of the hydrogen concentration in the feed.

kept constant: 20% H_2 in He, 400°C, 300 ml/min flow rate of sweep gas. The average H_2 permeability increases by a factor of 2 upon an increase in the flow of a factor of 3.3 (Fig. 7). From computational fluid dynamics calculations it is expected that the mass transfer resistance would reduce the permeability by 30% only. Therefore, it is expected that more processes than only mass transfer in the gas phase are involved in the variation of H_2 permeability with feed flow rate. The migration of Ag might have an amplifying effect on the permeability, as a small change in H_2 permeability causes a change in the Pd/Ag equilibrium, which subsequently has an effect on the hydrogen permeability. In addition, impurities at the membrane surface might be removed by the larger feed flow.

In Fig. 8, the measured fluxes are compared to fluxes found in the literature. The comparison is given in two different flux definitions; in the left graph the flux per driving force is defined as mol $H_2/m^2 \cdot s \cdot bar$, while in the right graph it is expressed per $bar^{0.5}$. In the temperature range measured here, the fluxes per driving force are high as compared to the values found in the literature. Extrapolation of our results to higher temperatures yields identical fluxes as found by

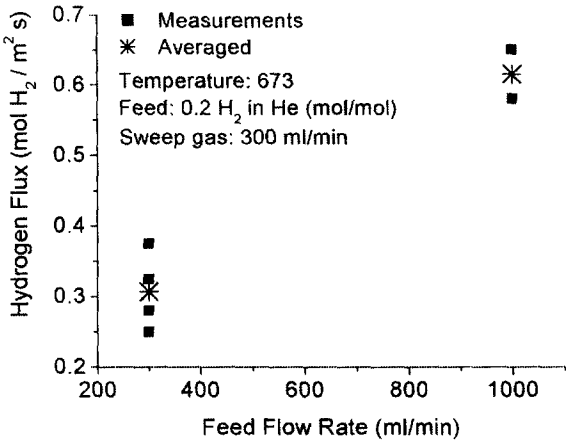

Fig. 7. Hydrogen permeability as function of the feed flow rate.

Franz and Jensen [14], also using micro-system technology to fabricate the membranes.

From each sample taken, it is possible to detect a leak during the permeation experiment from the He concentration. However, no Helium was found during the experiments. Therefore, in order to calculate a minimum selectivity of H_2 over Helium, the detection limit of the GC for He is used as the maximum He concentration. At a H_2

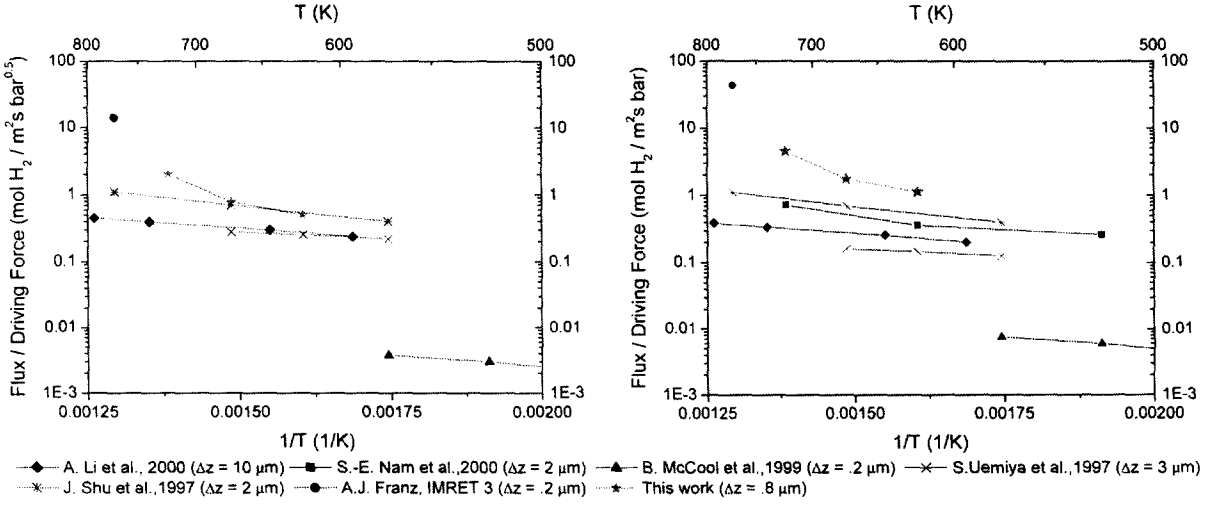

Fig. 8. Fluxes compared to literature data.

mol fraction of 0.2 in the feed, the calculated minimum selectivities are 30 and 1500 at 350°C and 450°C, respectively. These calculated values could have been much higher when a GC with lower He detection limit was used. Therefore, it is impossible to give a quantitative discussion about the presence of pinholes.

Acknowledgements

This research was supported by the Dutch Science and Technology Foundation (STW), ABB Lummus Global, Aquamarijn and DSM.

References

[1] M. Sheintuch and R.M. Dessau, Observations, modeling and optimization of yield, selectivity and activity during dehydrogenation of isobutane and propane in a Pd membrane reactor, Chem. Eng. Sci., 51 (1996) 535–547.

[2] E. Gobina and R. Hughes, Reaction assisted hydrogen transport during catalytic dehydrogenation in a membrane reactor, Appl. Catal. A: General, 137 (1996) 119–127.

[3] J.P. Collins, R.W. Schwartz, R. Sehgal, T.L. Ward, C.J. Brinker, G.P. Hagen and C.A. Udovich, Catalytic dehydrogenation of propane in hydrogen permselective membrane reactors, Ind. Eng. Chem. Res., 35 (1996) 4398–4405.

[4] Y. Yildirim, E. Gobina and R. Hughes, An experimental evaluation of high-temperature composite membrane systems for propane dehydrogenation, J. Membr. Sci., 135 (1997) 107–115.

[5] R. Dittmeyer, V. Höllein and K. Daub, Membrane reactors for hydrogenation and dehydrogenation processes based on supported palladium, J. Mol. Catal. A: Chemical, 173 (2001) 135–184.

[6] X.L. Pan, G.X. Xiong, S.S. Sheng, N. Stroh, H. Brunner, Thin dense Pd membranes on α-Al_2O_3 hollow fibers, Chem. Commun., 24 (2001) 2536–2537.

[7] S. Goto, S. Assabumrungrat, T. Tagawa and P. Praserthdam, The effect of direction of hydrogen permeation on the rate through a composited palladium membrane, J. Membr. Sci., 175 (2000) 19–24.

[8] S. Tosti, L. Bettinali, S. Castelli, F. Sarto, S. Scaglione and V. Violante, Sputtered, electroless, and rolled palladium-ceramic membranes, J. Membr. Sci., 196 (2000) 241–249.

[9] J.L. Vossen and W. Kern, Thin Film Processing II, Academic Press, Inc., 1991.

[10] H.D.Tong, F.C.Gielens, M.C.Elwenspoek, in press.

[11] T.L. Ward and T. Dao, Model of hydrogen permeation behavior in palladium membranes, J. Membr. Sci., 153 (1999) 211–231.

[12] F.J. Kuijers, V. Ponec, The surface composition of Pd-Ag alloys, J. Catal., 60 (1979) 100–109.

[13] J. Shu, B.E.W. Bongondo, B.P.A. Grandjean, A. Adnot and S. Kaliaguine, Surface segregation of Pd-Ag membranes upon hydrogen permeation, Surf. Sci., 291 (1993) 129–138.

[14] A.J. Frank, K.F. Jensen and M.A. Schmidt, Proc. Conf. IMRET3, (2000) 267–276.

[15] J. Shu, B.P.A. Grandjean, S. Kaliaguine, P. Ciavrella, A. Giroir and J.-A. Dalmon, Gas permeation and isobutane dehydrogenation over very thin Pd/ceramic membranes, Can. J. Chem. Eng., 75 (1997) 712–720.

[16] S. Uemiya, M. Kajiwara and T. Kojima, Composite membranes of group VIII metal supported on a porous alumina, AIChE J., 43 (1997) 2715–2723.

[17] B. McCool, G. Xomeritakis and Y.S. Lin, Composition control and hydrogen permeation characteristics of sputter deposited palladium-silver membranes, J. Membr. Sci., 161 (1999) 67–76.

[18] S.E. Nam and K-H. Lee, A study on the palladium/nickel composite membrane by vacuum electrodeposition, J. Membr. Sci., 170 (2000) 91–99.

[19] A. Li, W. Liang and R. Hughes, Fabrication of dense palladium composite membranes for hydrogen separation, Catal. Today, 56 (2000) 45–51.